Faraday Discuss. Chem. Soc., 1987, **83**, 47–57

Particle Diffusion in Concentrated Dispersions

William van Megen and Sylvia M. Underwood†
Department of Applied Physics, Royal Melbourne Institute of Technology, Melbourne, Victoria, Australia

Ronald H. Ottewill* and Neal St. J. Williams
School of Chemistry, University of Bristol, Cantock's Close, Bristol BS8 1TS

Peter N. Pusey
Royal Signals and Radar Establishment, Malvern, Worcestershire WR14 3PS

Three dynamic light scattering experiments on concentrated non-aqueous dispersions of spherical particles are discussed. The first two consist of measurements of the diffusion of tracer particles in different systems. In each case, host dispersions were rendered transparent by adjusting the refractive index of the dispersion medium to be the same as that of the particles. Trace amounts of particles of different refractive index, but of similar size and sterically stabilized by the same polymeric layer as the host particles, were added to the host dispersion. Thus the tracer particles provided the dominant incoherent light scattering. The measured correlation functions were analysed to provide particle mean-square displacements from which short- and long-time self-diffusion coefficients were obtained. In the third experiment the coherent scattering from concentrated dispersions of a single particle species was studied up to very high concentrations. Clear evidence of the glass transition, recently predicted, was found.

1. Introduction

In this paper we describe three separate dynamic light scattering (d.l.s.) experiments designed to elucidate the nature of diffusion processes occurring in concentrated colloidal dispersions of spherical particles (polymer colloids).

In the first two experiments the self-motion of individual particles, at dispersion volume fractions up to *ca.* 0.50, was studied by tracer techniques (incoherent scattering). In the third experiment collective particle motions (coherent scattering) were studied at higher concentrations where a long-lived amorphous or glassy phase was observed.

In a system of identical interacting particles d.l.s. measures the collective particle motions. However, a simple and important dynamic property of such a system is the average motion of a single particle. An obvious way to measure this self-motion by light scattering is to match the refractive index of the dispersion medium to that of the particles and to add to the resulting transparent (non-scattering) 'host' dispersion a small concentration of 'tracer' particles. The latter should have a different refractive index, but the same size and interaction properties as the particles of the host dispersion. This principle is exploited in the first two experiments where systems different in several respects were studied in Bristol and Melbourne. At Bristol the system consisted of poly(methylmethacrylate) (PMMA) tracer particles in a host dispersion of poly(vinylacetate) (PVA) particles index-matched in a mixture of *cis*- and *trans*-decalin; the average diameter of both types of particle was 168 nm. At Melbourne PMMA particles of

† Permanent address: Dulux Australia Limited, Clayton, Victoria 3168, Australia.

diameter 660 nm, index-matched in a mixture of decalin and carbon disulphide, were used as the host particles; the tracer particles were silica of a similar size. In all cases, however, the particles were stabilized by a comb polymer with essentially a PMMA backbone and 'teeth' of poly(12-hydroxystearic acid) (PHS). Because of the large difference in particle size between the two experiments different regimes of particle motion are probed, *i.e.* motions on small and large spatial scales relative to the particle diameters.

The third experiment (Malvern) used PMMA/PHS particles (average diameter 250 nm), dispersed in a mixture of decalin and carbon disulphide. The refractive index was chosen to be slightly different from the particles in order to provide reasonably strong coherent scattering.

2. Theory

Dynamic light scattering measures the normalized time correlation function of the intensity, I, of scattered light, where t is the correlation delay time,

$$g^{(2)}(t) = \langle I(0)I(t)\rangle / \langle I\rangle^2 \tag{1}$$

and the angular brackets represent an average over starting times '0'. If the light has Gaussian statistics the measured normalized dynamic structure factor is given by

$$C\frac{F^{\mathrm{M}}(Q,t)}{F^{\mathrm{M}}(Q,0)} = [g^{(2)}(t)-1]^{1/2} \tag{2}$$

where C is a constant which is determined by experimental factors such as the finite size of the detector.[1] The assumption of Gaussian statistics applies to all systems discussed in this paper except the very dense metastable suspensions described in section 4.2. For a suspension of spherical particles the measured dynamic structure factor is[2]

$$F^{\mathrm{M}}(Q,t) = \sum_{j,k=1}^{N} \langle b_j(Q)b_k(Q)\exp\{\mathrm{i}\boldsymbol{Q}\cdot[\boldsymbol{r}_j(0)-\boldsymbol{r}_k(t)]\}\rangle. \tag{3}$$

Here $b_k(Q)$ is the scattering amplitude of the kth particle and $\boldsymbol{r}_k(t)$ its position at time t, N is the number of particles in the scattering volume and $Q = 4\pi n \sin(\theta/2)/\lambda_0$ is the scattering vector (where n is the refractive index of the dispersion, λ_0 the wavelength of the light *in vacuo* and θ the scattering angle). In the 'ideal' case, where the particles differ only in their scattering amplitudes, there is no correlation between b_j and r_j so that eqn (3) reduces to[2]

$$F^{\mathrm{M}}(Q,t) = N(\overline{b^2}-\bar{b}^2)F_{\mathrm{s}}(Q,t) + N\bar{b}^2F(Q,t) \tag{4}$$

where

$$F_{\mathrm{s}}(Q,t) = \langle\exp\{\mathrm{i}\boldsymbol{Q}\cdot[\boldsymbol{r}(0)-\boldsymbol{r}(t)]\}\rangle \tag{5}$$

is the self-(incoherent) dynamic structure factor,

$$F(Q,t) = N^{-1}\sum_{j,k=1}^{N}\langle\exp\{\mathrm{i}\boldsymbol{Q}\cdot[\boldsymbol{r}_j(0)-\boldsymbol{r}_k(t)]\}\rangle \tag{6}$$

is the full (coherent) dynamic structure factor and

$$\overline{b^m} = N^{-1}\sum_{j=1}^{N} b_j^m. \tag{7}$$

$F(Q,t)$ describes the dynamics of the spatial Fourier component (of wavenumber Q) of fluctuations in the number density of particles; $S(Q) \equiv F(Q,0)$ is the static structure factor.

If we further assume that the spheres are optically homogeneous, with particle j having refractive index n_j, then (in the Rayleigh–Gans–Debye approximation[3])

$$b_j(Q) = V(n_j - n_0)f(Q) \tag{8}$$

where V is the volume of the particle, n_0 the refractive index of the dispersion medium and $f(Q)$ is the scattering amplitude normalized such that $f(0) = 1$; thus the form factor $P(Q) \equiv f^2(Q)$. Therefore, in order to obtain F_s in a d.l.s. experiment a refractive index matching condition is required such that

$$\overline{b(Q)} = Vf(Q)N^{-1} \sum_{j=1}^{N} (n_j - n_0) = 0 \tag{9}$$

which implies

$$\overline{b^2(Q)} - \overline{b(Q)}^2 = V^2 P(Q) N^{-1} \sum_{j=1}^{N} (n_j^2 - n_0^2). \tag{10}$$

In the particular case of only two types of particle with refractive indices n_1 and n_2 at relative number concentrations α and $1-\alpha$, index-matching [eqn (9)] implies

$$\alpha n_1 + (1-\alpha)n_2 = n_0 \tag{11}$$

so that

$$\overline{b^2(Q)} - \overline{b(Q)}^2 = V^2 P(Q)\alpha(1-\alpha)(n_1 - n_2)^2. \tag{12}$$

Thus the refractive index of the suspension medium and the composition of the suspension can be adjusted to provide strong side incoherent scattering. Note that in this ideal situation α does not need to be small. However, in practice there can be distinct advantages in taking $\alpha \ll 1$, *i.e.* performing a genuine tracer experiment. In this case we take $b_2(Q) = 0$ (*i.e.* $n_2 = n_0$) so that the summation in eqn (3) runs only over particles of type 1; if the latter are present in trace amounts ($N_1 \ll N$) eqn (3) reduces to

$$\begin{aligned} F^M(Q, t) &= \sum_{j=1}^{N_1} b_j^2(Q)\langle \exp[i\boldsymbol{Q} \cdot \Delta \boldsymbol{r}_j(t)]\rangle \\ &= \sum_{j=1}^{N_1} b_j^2(Q) F_{s,j}(Q, t) \end{aligned} \tag{13}$$

where $F_{s,j}(Q, t)$ is the self-dynamic structure factor of the jth tracer particle and its displacement $\Delta \boldsymbol{r}_j(t) \equiv \boldsymbol{r}_j(t) - \boldsymbol{r}_j(0)$. If the tracer particles are monodisperse the normalized (measured) dynamic structure factor reduces to $F_s(Q, t)$. The advantage of this approach is that F_s is less sensitive to artefacts introduced by optical inhomogeneities and polydispersity of the particles. In particular, in this situation polydispersity of the host particles does not affect the light scattering directly and only enters through its effect on the average motion of the tracer particles.

For a monodisperse system the self-dynamic structure can be written[4]

$$F_s(Q, t) = \exp[-Q^2\langle \Delta r^2(t)\rangle/6] \times \{1 + \alpha_2(t)[Q^2\langle \Delta r^2(t)\rangle/6]^2 + \cdots\} \tag{14}$$

where α_2 *etc.* are functions which describe the non-Gaussian statistical properties of the displacement $\Delta \boldsymbol{r}(t)$. From the mean-square displacements, $\langle \Delta r^2(t)\rangle$, one can obtain self-diffusion coefficients in the short- and long-time limits:[2,5]

$$D_S^s = \lim_{t \to 0} \langle \Delta r^2(t)\rangle/6t \tag{15}$$

and

$$D_L^s = \lim_{t \to \infty} \langle \Delta r^2(t)\rangle/6t. \tag{16}$$

Table 1. Details of latices

system	diameter/nm e.m.	diameter/nm d.l.s.	polydispersity	designation
PVA	128	166 ± 4	25%	SPVA/35
PMMA/1	141	170 ± 4	15%	SPSO/22
PMMA/2	—	660 ± 10	4%	SMU/1
PMMA/3	—	250 ± 10	15%	SMU/6
silica		630 ± 10	6%	SILA

Here D_S^s is the coefficient associated with (local) particle motion over distances much smaller than the particle radius, whereas D_L^s describes motion over macroscopic distances. D_S^s is obtained from the initial decay of $F_s(Q, t)$ at all scattering vectors whilst D_L^s is obtained from the long-time behaviour of F_s only in the limit of small scattering vectors where non-Gaussian terms are unimportant [eqn (14)].[2,5]

The work described in section 4.2 is concerned with a suspension showing significant size polydispersity but little optical polydispersity. It has been argued[6] that in this case $F^M(Q, t)$ [eqn (3)] can again be written as the sum of the averaged coherent and incoherent terms whose amplitudes are complicated functions of both the particle size distribution and concentration. However, for measurements near the main peak in the (static) structure factor, the case considered here, the interpretation of the data will assume that the strong coherent scattering dominates any incoherent scattering. Thus $F^M(Q, t)$ will be assumed to provide a reasonable estimate of the full dynamic structure factor given in eqn (6).

3. Experimental

Materials

The PMMA latices were prepared by dispersion polymerization using the method previously described[7,8] and the PVA latices were prepared by a similar process.[9] The particles were stabilized by a comb stabilizer which consisted of PHS 'teeth' grafted to a poly(glycidyl methacrylate)–PMMA backbone.[8] Silica particles were prepared from tetraethylorthosilicate in an ethanol–water medium using the method of Stöber *et al.*;[10] the particles were subsequently stabilized by physical adsorption of the same comb polymer as that used for the PMMA and PVA particles. The particle diameters determined by d.l.s. in dilute suspension and, in some cases, electron microscopy (carbon replicas), along with their polydispersities (standard deviation of the size distribution divided by the mean), are listed in table 1.

After preparation the particle dispersions were cleaned by centrifugation, removal of the supernatant and redispersing in the required filtered solvents; this process was repeated several times. In addition, latices of the smallest particles (*i.e.* PVA and PMMA/1) were filtered through Nucleopore membranes.

Preparation of Optically Matched Dispersions

The PVA particles, with an average refractive index of 1.471, could be precisely optically matched (rendered transparent) by a mixture of *cis*-decalin ($n = 1.481$) and *trans*-decalin ($n = 1.469$). Optimum match conditions were achieved by adjusting the liquid composition until the intensity of the (laser) light scattered by the dispersion was a minimum. A similar procedure was followed for PMMA/2 and PMMA/3 using a mixture of decalin

(mixture of *cis* and *trans*, $n \approx 1.48$) and carbon disulphide ($n = 1.63$) for an index-matching liquid. Owing to the significant (different) optical dispersions for PMMA and the decalin-CS_2 mixture, the matchpoint in these dispersions displays a greater wavelength dependence than for the PVA dispersions. Both PMMA/2 and PMMA/3 were optimally matched for the blue ($\lambda = 488$ nm) laser line, but they still provided strong scattering at larger wavelengths (*e.g.* $\lambda = 647$ nm).

The (index-matched) dispersions were brought to the required particle concentration by centrifugation, removal of a weighed amount of clear supernatant and redispersal of the particles by a combination of rapid agitation and slow tumbling.

The dynamic light scattering experiments were performed using standard photon correlation equipment.

4. Results and Discussion

4.1 Tracer Experiments

The first of two tracer systems (T1) was prepared by adding to the transparent PVA host dispersion, PMMA/1, particles at relative PMMA:PVA concentration 1:43. The second tracer system (T2) was composed of *ca.* one silica particle for every 500 PMMA/2 host particles. In both cases the tracer particles were dispersed in the same liquid mixture as the host particles prior to their addition to the host dispersion. Since the host and tracer particles have about the same diameter (see table 1) and carry the same stabilizing polymer coating, it may be assumed that the (repulsive) interactions between the host particles and the host and tracer particles are essentially identical.

In order to facilitate presentation of the results below, two further details need to be discussed. First, the PMMA/1 and PVA volume fractions were determined from weight-fraction analysis of the dispersions; the conversion from weight fraction to effective interaction volume fraction was accomplished taking the densities of the components and assuming a value of 9 nm for the stabilizer layer thickness. In the case of PMMA/2 this was accomplished by equating the core volume fraction (ϕ_c) at which crystallization commenced with the known freezing volume fraction ($\phi_f = 0.494$) of hard spheres. This procedure, which is fully discussed in ref. (5) and (11), gives the effective volume fraction

$$\phi_E = 1.125\phi_c. \tag{17}$$

This gives an effective hard-sphere radius *ca.* 13 nm larger than the PMMA/2 core radius. The difference between this value (13 nm) and the expected average extended chain length of the adsorbed polymer (9 nm) may be due to some swelling of the particle cores as a result of CS_2 absorption in the CS_2–decalin mixtures. A similar procedure for this conversion to ϕ_E is precluded for PVA owing to its small particle diameter and significant polydispersity.

The second point concerns the non-Gaussian terms in eqn (14), *i.e.* the interpretation of F_s. The wavenumbers at which system T1 (PMMA/1 in PVA) was studied were below the location of the first maximum,[12] Q_m, in the static structure factor and too small for the non-Gaussian terms to be appreciable. Therefore, in this case the Gaussian approximation to F_s, namely,

$$F_s(Q, t) = \exp[-Q^2\langle\Delta r^2(t)\rangle/6] \tag{18}$$

should be reasonable. By virtue of the larger particle diameters, system T2 (silica in PMMA/2) was studied at wavenumbers well beyond Q_m, thereby ensuring that the Gaussian part of F_s has decayed to negligible values before appreciable growth of the non-Gaussian terms. Thus, eqn (18) has also been used in interpreting the data for system T2. Recent computations of F_s by Brownian dynamics on concentrated dispersions suggest that non-Gaussian effects are most noticeable at $Q \approx Q_m$.[13] Further support

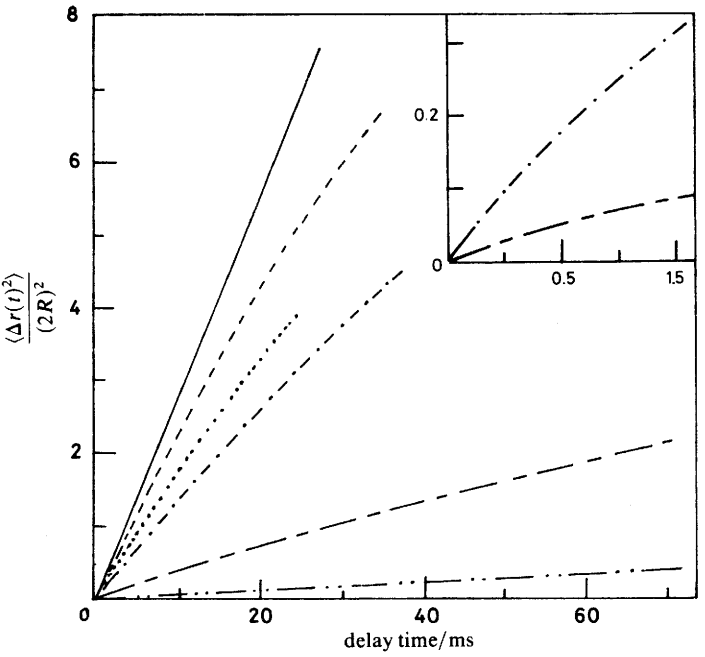

Fig. 1. Mean-square displacements in terms of the particle diameter $2R$, for tracer system T1 (PMMA/1 in PVA) showing free diffusion (——) and results for (effective) volume fractions $\phi_E = 0.04$ (– – –), $\phi_E = 0.11$ (· · · · ·), $\phi_E = 0.20$ (· · –), $\phi_E = 0.41$ (— – —), $\phi_E = 0.50$ (— · —). The inset shows the short-time behaviour at $\phi_E = 0.20$ (— · · —) and $\phi_E = 0.41$ (— – —).

for the above assumption is provided by the fact that any wavenumber dependence of the measured F_s was within the random errors normally expected for d.l.s. measurements.

Fig. 1 and 2 show the mean-square displacements, in units of the particle diameter, derived from eqn (18) as functions of time for the systems T1 and T2. The results obtained are curved and show increasing deviation from free diffusion as ϕ_E is increased. The inset in fig. 1 shows the behaviour at shorter times for the system T1 at $\phi_E = 0.20$ and 0.41. As expected, in view of the different particle sizes in the two systems, and evident from the ordinate scales of fig. 1 and 2, quite different relative spatial scales are probed in the two cases. In fig. 2 the curvature of the plots is associated with the transition from short-time (local) motion to long-time (large-distance) diffusion. However, the asymptotic long-time behaviour has not been fully reached before F_s has decayed into the noise. On the other hand, in the main part of fig. 1 the long-time regime should have been reached and linear dependence of the mean-square displacement found. The residual curvature evident in fig. 1 is probably caused by the significant polydispersity of the tracer particles in system T1 (see table 1).

In order to obtain the short-time diffusion coefficients, D_S^s, defined in eqn (15) and plotted in fig. 3, self-dynamic structure factors, measured at short times, were analysed by the method of cumulants.[14] The resulting values of D_S^s for the two tracer systems are in good agreement; they also agree, within experimental error, with results (also plotted in fig. 3) obtained earlier from the large-wavenumber coherent scattering by dispersions of significantly larger PMMA particles.[15] The theoretical prediction of Beenakker and Mazur,[16] based on a partial summation of the many-body hydrodynamic interactions, is also shown in fig. 3; slight differences between experiment and theory are evident.

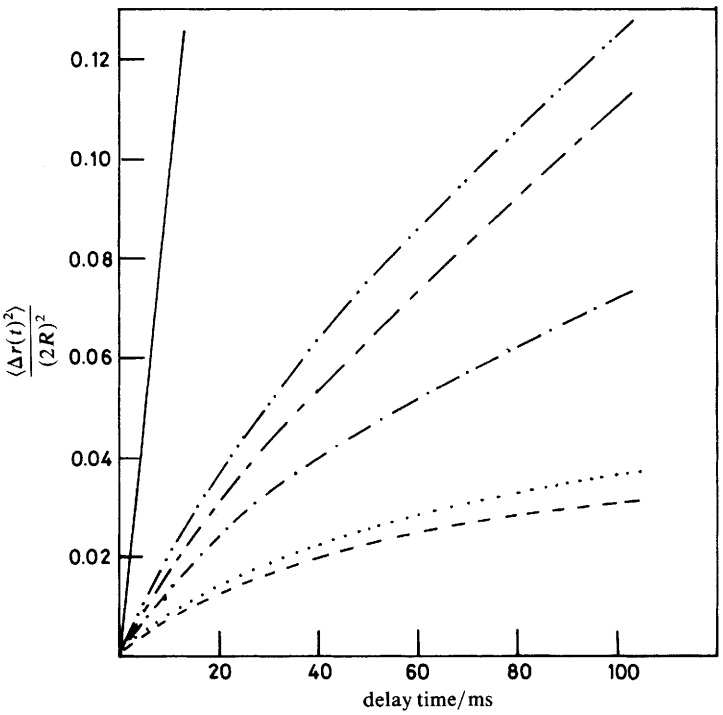

Fig. 2. Mean-square displacements for tracer system T2 (silica in PMMA/2) showing free diffusion (——) and results for (effective) volume fractions $\phi_E = 0.38$ (— · · —), $\phi_E = 0.41$ (— - - —), $\phi_E = 0.44$ (— · —), $\phi_E = 0.49$ (· · · ·) and $\phi_E = 0.54$ (- - -). Note that the last two curves, for $\phi_E = 0.49$ and 0.54, represent results for coexisting disordered and crystalline phases.

The long-time tracer diffusion coefficients D_L^s, defined in eqn (16) and plotted in fig. 4, were obtained by fitting a single exponential to the long-time behaviour of F_s. In the analysis of the data of system T1 this involved omitting the first quarter of the data, whereas for T2, roughly the first half was omitted. However, as mentioned above, the macroscopic diffusive limit is not fully reached for system T2, so that the values of D_L^s obtained from these data are likely to be overestimated; such a trend is evident in fig. 4. The present results are in good agreement with the earlier data of Kops-Werkhoven and Fijnaut,[17] also plotted in fig. 4. In addition, fig. 4 shows a trace summarising the short-time results D_S^s of fig. 3. Clearly, local diffusion of a particle within its current nearest-neighbour cage (as represented by D_S^s) is, at high concentrations, many times faster than its motion (represented by D_L^s) over distances comparable with or larger than its diameter. The approach of D_L^s to zero at $\phi_E \approx 0.55$ is consistent with the onset of crystallization.[11]

4.2. The Glass Transition

In the previous section we discussed single-particle diffusion in both the fluid and crystalline phases of suspensions. Whilst at volume fractions beyond the melting concentration ($\phi_E = 0.545$) the thermodynamically stable phase is crystalline, recent work[11] has shown that it is possible to prepare suspensions which remain in an amorphous (or glassy) state for very long times. Such behaviour has also recently been found in computer simulation[18–20] and theoretical models[21,22] of simple atomic fluids. Since it is

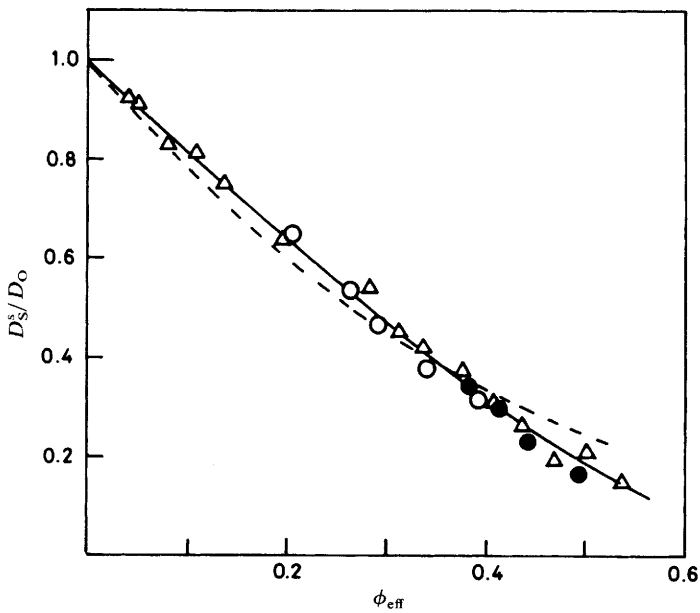

Fig. 3. Short-time self-diffusion coefficients D_S^s (expressed in units of the free particle diffusion constant D_O) defined by eqn (15), *vs.* effective volume fraction, as obtained from tracer systems T1 (△) and T2 (●). Shown also are the data from ref. (15) (○) and the theoretical result of ref. (16) (- - -).

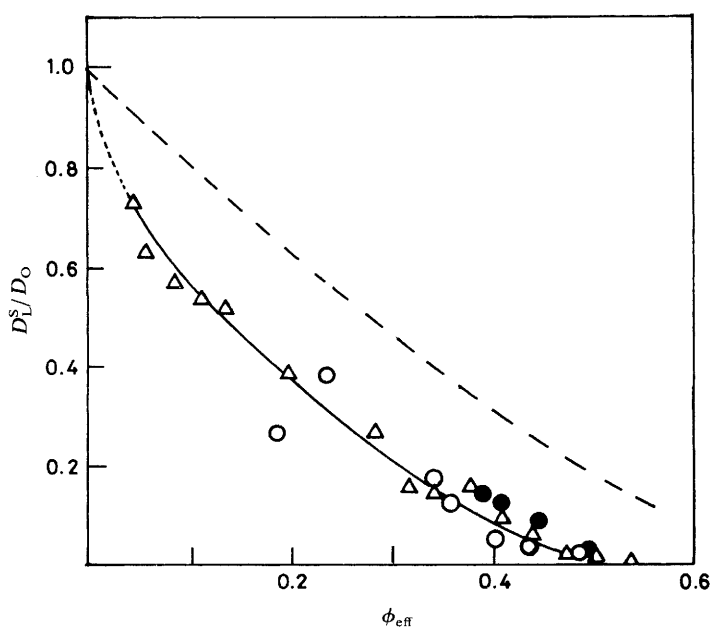

Fig. 4. Long-time diffusion coefficients, D_L^s, defined by eqn (16), *vs.* effective volume fraction, as obtained from tracer systems T1 (△) and T2 (●). Shown also are the data from ref. (17) (○). The dashed curve represents a trace through the results for D_S^s in fig. 3.

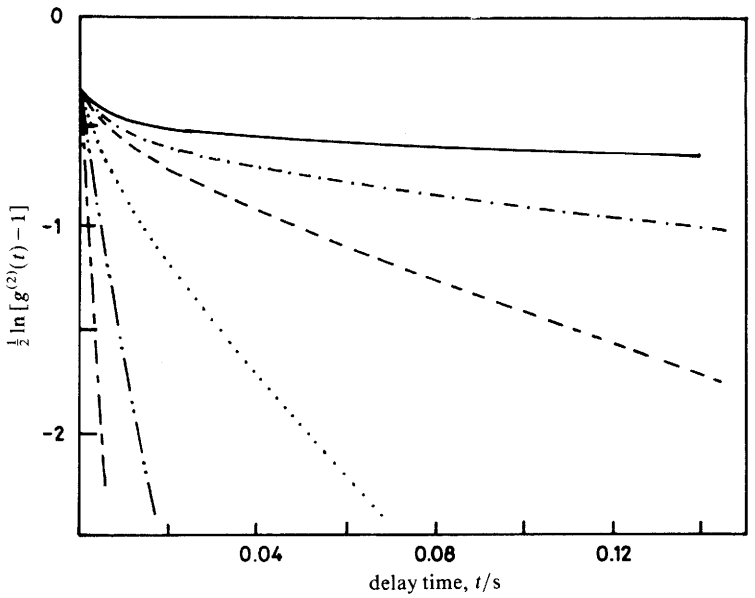

Fig. 5. Logarithm of the intensity autocorrelation function *vs.* time for dispersions of PMMA/3. Sample 1, $\phi_c = 0.196$ (— - —); sample 2, $\phi_c = 0.262$ (— · · —); sample 3, $\phi_c = 0.308$ (· · · · ·); sample 4, $\phi_c = 0.331$ (- - -); the 'coexisting liquid' of sample 5, (- · -), studied after phase separation had occurred (see text); sample 5, $\phi_c = 0.349$ (——).

impossible to compress (or quench) atomic fluids sufficiently rapidly to bypass crystallization, concentrated suspensions of particles, in which the diffusive motions are slower by a factor of *ca.* 10^9, constitute possibly the only real systems composed of spherical units in which the nature of the glass transition can be studied.

Here we report measurements of the dynamic light scattering near the main peak in the structure factor (*i.e.* near Q_m) by particle suspensions at concentrations up to $\phi_E \approx 0.60$. The reason for choosing this particular wavevector is to allow us to compare results with recent molecular dynamics studies by Ullo and Yip[20] on a fluid of slightly soft atoms.

In order to measure the very slow motion occurring at high particle concentrations in a reasonable length of time we used PMMA particles of roughly half the size (PMMA/3, see table 1) of those used in earlier work.[11] Unfortunately, to date it has not proved possible to prepare such small PMMA particles with narrow size distributions, and for the particles used here the polydispersity was *ca.* 15%.

In fig. 5 and 6, we show plots of $\frac{1}{2}\ln[g^{(2)}(t)-1]$ *vs.* t at $Q \approx 2.61 \times 10^5\ \mathrm{cm}^{-1}$ for a range of core volume fractions ϕ_c, determined in the same manner as for PMMA/2 (section 4.1). In general, the correlation functions show a relatively rapid initial decay followed by a slower decay at long times, the latter becoming essentially zero at the highest volume fractions studied. This vanishing of the long-time decay rate is precisely the behaviour found in the theoretical treatments of Leutheusser[21] and Bengtzelius *et al.*[22] and in the computer simulations of Ullo and Yip.[20] The interpretation given to this observation is that at the glass transition the particles become trapped by their local environments. While the particles still retain some freedom for local motions within their nearest-neighbour cages, as indicated by the rapid initial decay of the correlation functions, that part of the density fluctuation corresponding to longer-ranged particle translation has effectively been frozen in.

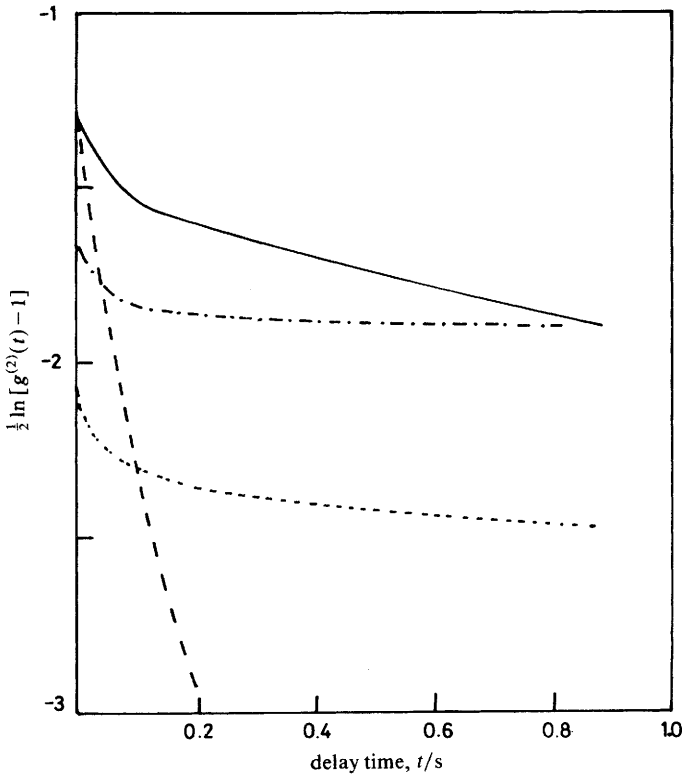

Fig. 6. Logarithm of the intensity autocorrelation fraction *vs.* time for dispersions of PMMA/3. Sample 4, $\phi_c = 0.331$ (- - -); sample 5, $\phi_c = 0.349$ (——); sample 6, $\phi_c = 0.378$ (— · —); sample 7, $\phi_c = 0.408$ (· · · ·).

In the case where the density fluctuations are partly frozen in, the light scattered into a fixed detector no longer has Gaussian statistics. Thus, the scattered intensity consists of a fluctuating component associated with the local motions and an essentially constant component associated with the frozen density fluctuations. This leads to a reduction in the magnitude of the intensity fluctuations, $(\langle I^2\rangle/\langle I\rangle^2)-1$, measured in an experiment of finite duration. The zero-time value of $g^{(2)}(t)-1$ is a measure of $(\langle I^2\rangle/\langle I\rangle^2)-1$ [see eqn (1)]. In fig. 6 we note that, whereas sample 5 shows the full modulation of the intensity, a marked reduction of this fluctuation magnitude is observed for samples 6 and 7. To be precise, the light scattered by sample 5 undergoes many (Gaussian) fluctuations in the duration of a measurement (10^3 s). However, the reduced magnitude of fluctuations measured in the intensity scattered by samples 6 and 7 implies unambiguously, if not the existence of permanently frozen-in density fluctuations, at least the presence of fluctuation times much longer than 10^3 s.

For various reasons, for example the significant polydispersity of the samples, we will not, in this preliminary report, attempt a quantitative comparison with the molecular dynamics results of Ullo and Yip.[20] However, our findings are in good qualitative agreement with their computer simulation data [compare fig. 5 with fig. 3 of ref. (20)].

It remains to determine the effective volume fraction at which the glass transition occurs. In previous work on samples which showed a relatively rapid and reproducible crystallization[11] we determined freezing and melting concentrations and, by reference to a hard-sphere model, were able to obtain effective hard-sphere volume fractions ϕ_E

(see section 4.1). Probably owing to their large polydispersity,[23,24] the present samples did not exhibit the rapid crystallization characteristic of (almost) monodisperse systems. However, after several days, sample 5 had separated into a polycrystalline phase, occupying *ca.* 80% of the total volume, and a fluid-like phase. Thus, taking freezing and melting volume fractions of hard spheres to be 0.494 and 0.545, respectively,[15] we calculate the effective hard-sphere volume fraction of sample 5 to be $\phi_E \approx 0.535$. Then sample 6, which is the first to show relaxation times $> 10^3$ s, has an effective volume fraction $\phi_E \approx 0.575$. In view of the significant uncertainties in this determination of ϕ_E for a polydisperse system, this result for the onset of the glass transition is in reasonable agreement with values found in previous experimental work[11] and computer simulations,[18,19] which lie in the range $0.56 \leqslant \phi_E \leqslant 0.60$.

In conclusion the above observations clearly indicate the formation of a long-lived dense metastable amorphous state in particle suspensions (and, by implication, in a simple liquid). We are currently investigating this behaviour in greater detail with less polydisperse samples.

References

1 E. Jakeman, in *Photon Correlation and Light Beating Spectroscopy*, ed. H. Z. Cummins and E. R. Pike (Plenum Press, New York, 1974).
2 P. N. Pusey and R. J. A. Tough, in *Dynamic Light Scattering*, ed. R. Pecora (Plenum Press, New York, 1985).
3 M. Kerker, *The Scattering of Light* (Academic Press, New York, 1969).
4 B. R. A. Nijboer and A. Rahman, *Physica*, 1966, **32**, 415.
5 W. van Megen, S. M. Underwood and I. Snook, *J. Chem. Phys.*, 1986, **85**, 4065.
6 P. N. Pusey, H. M. Fijnaut and A. Vrij, *J. Chem. Phys.*, 1982, **77**, 4270.
7 *Dispersion Polymerization in Organic Media*, ed. K. E. J. Barrett (Wiley, London, 1975).
8 L. Antl, J. W. Goodwin, R. D. Hill, R. H. Ottewill, S. M. Owens, S. Papworth and J. A. Waters, *Colloid Surf.*, 1986, **17**, 67.
9 S. Papworth and R. H. Ottewill, to be published.
10 W. Stöber, A. Fink and E. Bohn, *J. Colloid Interface Sci.*, 1968, **26**, 62.
11 P. N. Pusey and W. van Megen, *Nature* (*London*), 1986, **320**, 340.
12 R. H. Ottewill and N. St. J. Williams, *Nature* (*London*), 1987, **325**, 232.
13 W. van Megen and I. Snook, to be published.
14 D. E. Koppel, *J. Chem. Phys.*, 1972, **57**, 4814.
15 P. N. Pusey and W. van Megen, *J. Phys.* (*Paris*), 1983, **44**, 258.
16 C. W. J. Beenakker and P. Mazur, *Physica*, 1984, **126A**, 349.
17 M. M. Kops-Werkhoven and H. M. Fijnaut, *J. Chem. Phys.*, 1981, **74**, 1618.
18 L. V. Woodcock, *Ann. N.Y. Acad. Sci.*, 1981, **37**, 274.
19 C. A. Angell, J. H. R. Clarke and L. V. Woodcock, *Adv. Chem. Phys.*, 1981, **48**, 397.
20 J. J. Ullo and S. Yip, *Phys. Rev. Lett.*, 1985, **54**, 1509.
21 E. Leutheusser, *Phys. Rev. A*, 1984, **29**, 2765.
22 U. Bengtzelius, W. Götze and A. Sjölander, *J. Phys. C*, 1984, **17**, 5915.
23 E. Dickinson and R. Parker, *J. Phys. Lett.*, 1985, **46**, C229.
24 J. L. Barrat and J. P. Hansen, *J. Phys.* (*Paris*), 1986, **47**, 1547.
25 W. G. Hoover and F. H. Ree, *J. Chem. Phys.*, 1968, **49**, 3609.

Received 5th January, 1987